Digest Journal of Nanomaterials and Biostructures Vol. 17, No. 3, July - September 2022, p. 899 - 912

Preparation of organic dye-modified calcium-aluminum layered double hydroxide powders and their cytotoxicity

C. Suwanchawalit[a], C. Deeleepojananan[a], N. Triamnak[b], P. Opanasopit[c],
S. Laksee[d], S. Suvokhiaw[a,*]
[a]*Department of Chemistry, Faculty of Science, Silpakorn University, Nakornpathom, Thailand 73000*
[b]*Department of Materials Science and Engineering, Faculty of Engineering and Industrial Technology, Silpakorn University, Nakhon Pathom, Thailand 73000*
[c]*Pharmaceutical Development of Green Innovations Group (PDGIG), Faculty of Pharmacy, Silpakorn University, Nakornpathom, Thailand 73000*
[d]*Nuclear Technology Research and Development Center, Thailand Institute of Nuclear Technology (Public Organization), Nakhon Nayok, Thailand 26120*

Incorporation of anions of indigo carmine dye and dodecyl sulphate to CaAl-layered double hydroxides (LDHs) has been carried out by the coprecipitation method. The effect of Ca^{2+}/Al^{3+} ions ratio on the color and photostability of the composites was studied. The FE-SEM images suggested that the CaAl/Indigo and CaAl/SDS/Indigo composites formed plate-like structure with loose stacking. XRD results showed that the CaAl-LDH were mainly composed of CaAl-hydrotalcites structure. The FT-IR spectra revealed the interaction between the sulfate groups and the LDH surface, and the functional groups of each counterpart were present. The UV-Vis absorption spectra of the CaAl/Indigo and CaAl/SDS/Indigo composites exhibited intense blue color. Furthermore, the CaAl/Indigo and CaAl/SDS/Indigo composites exhibited high photo-stability under UV irradiation. Cytotoxicity was then assessed using the methyl tetrazolium test (MTT) and the cell survival rate was determined. Cytotoxicity tests showed that most CaAl/Indigo and CaAl/SDS/Indigo composites are biocompatible to the GF cells except the SDS modified CaAl-hydrotalcites structure.

(Received April 20; 2022; Accepted August 14, 2022)

Keywords: LDHs; calcium-aluminum layer double hydroxide, Co-precipitation technique, anionic adsorption; Cytotoxicity

1. Introduction

Recently, a number of studies have focused on the preparation and characterization of organic-inorganic pigment composites [1-4]. Organic-inorganic pigment composites are colorants with pigment properties. They are usually obtained by precipitating dyes onto inorganic substrates such as calcium carbonate [5], alumina [6, 7], barium sulphate [8, 9], magnesium aluminum layered double hydroxides [1-3], producing hybrid organic-inorganic compounds. Hybrid organic-inorganic composites are widely used in plastics, coatings, textiles and fertilizers. Organic-inorganic composites have therefore attracted much attention from researchers interested in the design and fabrication of modern multifunctional coloring agents.

Layered double hydroxides (LDHs), also called hydrotalcite-like compounds, have a sandwich structure composed of a cation layer and an anion interlayer, both of which are quite tunable. In general, LDHs have been synthesized from various divalent ($M^{2+} = Mg^{2+}$, Zn^{2+}, Ni^{2+}) and trivalent cations ($M^{3+} = Al^{3+}$, Fe^{3+}, Cr^{3+}) in variable M^{2+}/M^{3+} mole ratios and accompanied by interlayer anions of diverse nature [10-12]. On the feature of LDHs host structure, guest organic molecules can be incorporated into the interlayer space to give hybrid materials with various

---

[*] Corresponding author: s_suntornsc@hotmail.com

https://doi.org/10.15251/DJNB.2022.173.899

functionalities which are suitable to be used in many applications such as pigments, optical devices, fillers in polymer composites, drug carriers, and catalysts.

In the current work, we propose new hybrid organic-inorganic pigment composites by incorporation of indigo carmine dye (IC) to CaAl-layered double hydroxides (CaAl-LDHs) by a coprecipitation method with different Ca/Al ratios. In this study, the CaAl/Indigo and CaAl/SDS/Indigo composites were characterized using X-ray diffraction (XRD), scanning electron microscopy (SEM) and Fourier transform infrared spectroscopy with attenuated total reflection (ATR-FTIR). The enhancement of stability of these compounds under UV irradiation was also evaluated.

Indigo carmine (IC), a deep blue dye widely used in the areas of textile dyeing and the coloring of plastics, has the structural formula as shown in Figure 1.

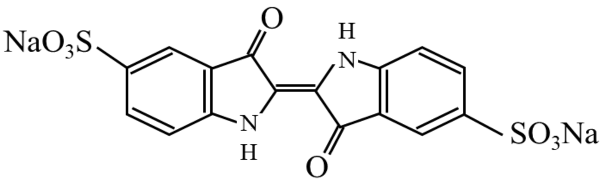

Fig. 1. The chemical structure of indigo carmine dye.

2. Materials and Methods

2.1 Materials

All chemicals were analytical grade and used as received without further purification. Aluminium chloride hexahydrate [$AlCl_3 \cdot 6H_2O$] (KemAus™, Australia), calcium chloride dihydrate [$CaCl_2 \cdot 2H_2O$] (Riedel-de Haen, Germany), Sodium dodecyl sulphate [$CH_3(CH_2)_{11}OSO_3Na$] (Loba Chemie, India), Indigo Carmine [$C_{16}H_9N_4Na_3O_9S_2$] (Sigma-Aldrich, USA) and sodium hydroxide (NaOH) (Merck, Germany) were used as starting materials.

2.2. Preparation of indigo carmine modified calcium-aluminum layer double hydroxide

2.2.1 Preparation of CaAl-LDHs

The CaAl-LDHs were prepared via the coprecipitation method as described in previous work [13-15]. Briefly, the mixed metal solution containing Ca^{2+} and Al^{3+} was prepared by dissolving $CaCl_2 \cdot 2H_2O$ and $AlCl_3 \cdot 6H_2O$ in deionized water and the final volume was then adjusted to 25.00 mL. NaOH solution (1.0 $mol \cdot L^{-1}$) was added dropwise into the mixed metal solution and stirring was continued at room temperature until the final pH was 11. The suspension was then aged at room temperature for 24 hours. The precipitate was separated by centrifugation at 4500 rpm for 10 minutes. Finally, it was washed three times with deionized water and then dried at 50°C for 24 hours. The as-synthesized products were ground and labelled as CaxAl-LDH (x is the molar ratio of Ca^{2+} and Al^{3+}, x = 2, 3 and 4).

Table 1. The code of samples.

Sample codes	The molar ratio of Ca^{2+}/Al^{3+}	Organic precursors
Ca2Al-LDH	2:1	-
Ca3Al-LDH	3:1	-
Ca4Al-LDH	4:1	-
Ca2Al/Indigo	2:1	indigo carmine
Ca3Al/Indigo	3:1	indigo carmine
Ca4Al/Indigo	4:1	indigo carmine
Ca2Al/SDS/Indigo	2:1	sodium dodecyl sulphate and indigo carmine
Ca3Al/SDS/Indigo	3:1	sodium dodecyl sulphate and indigo carmine
Ca4Al/SDS/Indigo	4:1	sodium dodecyl sulphate and indigo carmine

2.2.2. Preparation of organic dye-modified CaAl-LDH, CaAl/Indigo and CaAl/SDS/Indigo

The CaxAl/Indigo and CaxAl/SDS/Indigo were prepared by the coprecipitation method as described above with some modification. In brief, for CaxAl/SDS/Indigo, the mixed metal solution containing Ca^{2+} and Al^{3+} was prepared by dissolving $CaCl_2 \cdot 2H_2O$ and $AlCl_3 \cdot 6H_2O$ in deionized water and the final volume was then adjusted to 25.00 mL. Ten millilitres of a solution containing 0.25×10^{-3} mole sodium dodecyl sulphate (SDS) was slowly added into the mixed metal solution with continuous stirring. The obtained metal solution and NaOH solution (1.0 $mol \cdot L^{-1}$) were simultaneously added dropwise into 25.00 mL of 5.0×10^{-3} $mole \cdot L^{-1}$ indigo carmine solution with continuous stirring at room temperature. The final pH was adjusted to 11. The suspension was then aged at room temperature for 24 hours. The precipitate was separated by centrifugation at 4500 rpm for 10 minutes. Finally, it was washed three times with deionized water and then dried at 50°C for 24 hours. The as-synthesized products were ground and labelled as CaxAl/SDS/Indigo (x is the molar ratio of Ca^{2+} and Al^{3+}, x = 2, 3 and 4).

The CaxAl/Indigo samples were prepared in a similar manner to those of CaxAl/SDS/Indigo in the absence of the SDS solution.

2.3. Characterization of indigo-intercalated calcium-aluminum layer double hydroxide

The XRD patterns of all samples were collected with a Bruker D8 ADVANCE X-ray diffractometer in the 2θ range of 5 - 70 degrees with Cu Kα radiation operating at 35kV and 30 mA. The TESCAN MIRA3 FE-SEM was used to explore the morphology of the as-synthesized samples. Fourier transform infrared (FTIR) spectra were obtained with a Perkin Elmer Frontier™ FT-IR Spectrometer with attenuated total reflection (ATR). Ultraviolet-visible (UV-Vis) spectra were recorded on an Agilent Cary 60 UV-Vis Spectrophotometer in the range 360–820 nm. The $L^*a^*b^*$ and color difference (ΔE) of the as-synthesized materials aged under UV light were measured in terms of CIE 1976 $L^*a^*b^*$ using a Cary 60 UV-Vis Spectrophotometer with a remote fiber optic diffuse reflectance accessory (DRA). The color difference (ΔE) was calculated using the formula (1) [1]:

$$\Delta \mathrm{E} = \sqrt{\Delta L^{*2} + \Delta a^{*2} + \Delta b^{*2}} \quad (1)$$

where ΔL^* is the level of lightness or darkness, Δa^* is the relationship between redness and greenness, and Δb^* is the relationship between blueness and yellowness

2.4. Toxicity test of CaAl-SDS-LDH/Indigo carmine

2.4.1. Cell Culture

Gingival fibroblasts (GF) was obtained from explant cultures of human gingival tissue. GF cells were maintained in Dulbecco's modified Eagle's medium (DMEM; GIBCO) containing nonessential amino acids, penicillin-streptomycin (as above), Fungizone (0.5 g/mL), and 10% fetal bovine serum (FBS; Atlanta Biological). These tissues were incubated undisturbed for a week at 37°C, in humidified 95% air/5% CO_2, according to standard techniques, after which time the gingival fibroblasts were visible as outgrowths from the explanted tissue.

2.4.2. Cell viability assay

Cell viability was determined by the 3-(4, 5-dimethylthiazol-2-yl)-2,5-diphenyltetrazolium bromide (MTT) assay. GF cells were seeded in 96-well plates, medium in excess of 100 µL/well was removed, and 25 µL of MTT dye (5 µg/mL) in sterile phosphate-buffered saline (PBS) was added to each well. The plates were incubated for 3 h, during which time the mitochondria in the living cells converted the soluble yellow dye into an insoluble purple crystal. Th cells and dye were then solubilized by the addition of 10% sodium dodecyl sulfate (SDS) in 25% *N,N*-dimethylformamide, pH 3.6. The optical density of each well at 562 nm was determined by a microplate reader. Cell viability was then calculated using the following equation (2) [16]:

$$\text{Cell viability \%} = (A_s \,/\, Ac_{ontrol}) \times 100 \quad (2)$$

where A_s is the absorbance of cells treated under various conditions and $A_{control}$ is the absorbance of the cells in the standard medium.

4. Results and Discussion

4.1. Characterizations of indigo carmine-modified calcium-aluminum layer double hydroxide

Figure 2 shows the XRD patterns of Ca2Al-LDH, Ca3Al-LDH, and Ca4Al-LDH. It can be seen that, for all samples, the characteristic peaks of hydrocalumite (JCPDS 78-1219) were clearly observed at 2θ of about 13, 22, 23, 32 and 56 degrees [17]. However, the impurity phases of $CaCO_3$ (JCPDS No. 05-0586) and $Al(OH)_3$ (JCPDS No. 24-0006) were also found in all samples. This could be due to the carbonate contamination caused by carbon dioxide in the air during preparation. With a low molar ratio of Ca^{2+}/Al^{3+}, the hydrocalumite phase became less predominant, and the crystal sizes became smaller, consistent with the low intensities of (00l) reflections.

The XRD patterns of CaAl/Indigo and CaAl/SDS/Indigo are illustrated Figure 3. The characteristic reflections of hydrocalumite were found in all materials. The (00l) basal reflections of all samples were found at the same position with pristine CaAl-LDHs. This indicated that the organic counterparts could not intercalate into the interlayer of CaAl-LDHs and were bound at the surface of CaAl-LDHs instead. For the samples Ca2Al/Indigo, Ca3Al/Indigo, and Ca4Al/Indigo (Fig. 3 a-c), the intensity of (00l) peaks decreased with increasing molar ratios of Ca^{2+}/Al^{3+}. This was due to the fact that the higher layer charges led to stronger attraction forces between the layer cations and the interlayer anions resulting in a better arrangement of the interlayer anions and a higher degree of crystallinity in the materials. With decreasing layer charges (increasing molar ratio of Ca^{2+}/Al^{3+}), the arrangement of the interlayer anions became less predominant resulting in a lower degree of crystallinity.

This result is in good agreement with previous reports [18, 19]. The XRD patterns of Ca2Al/SDS/Indigo, Ca3Al/SDS/Indigo and Ca4Al/SDS/Indigo (Fig. 3(e) – (f)) showed that the predominant phase was hydrocalumite with a small amount of $CaCO_3$ impurity phase. This is obviously evident that the co-existence of indigo carmine dye and dodecyl sulphate ions in solution during the formation of CaAl-LDHs could provide the optimum environment for growing up the double layer of CaAl-LDHs, and the presence of SDS could prevent the formation of the impurity phases of $CaCO_3$ and $Al(OH)_3$ phases.

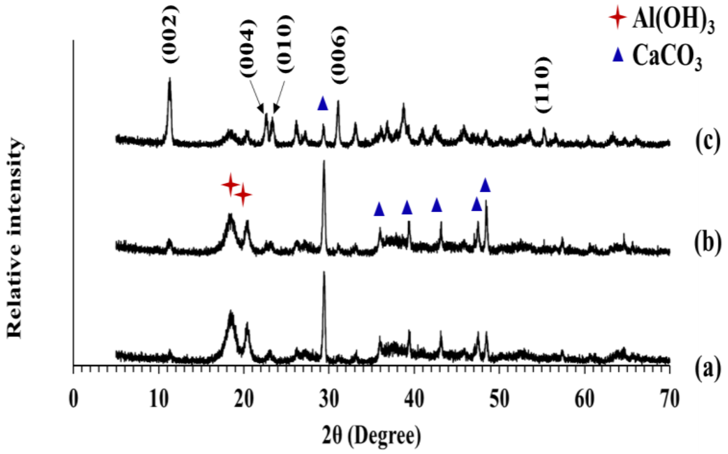

Fig. 2. XRD patterns of (a) Ca_2Al-LDH, (b) Ca_3Al-LDH and (c) Ca_4Al-LDH.

The SEM images of Ca_2Al-LDH, Ca_3Al-LDH and Ca_4Al-LDH (Fig. 4) showed a plate-like structure with loose packing. While CaAl-LDHs were plate-like particles, the indigo carmine powder (Fig. 4d) was found to be bulk and dense particles. Comparing to the bare CaAl-LDHs, the particle sizes of the organic modified CaAl-LDHs (Fig. 5) were larger with looser staking. The reason behind this could be that the indigo carmine and SDS could bind to the CaAl-LDHs surface and then restricted the assemble of LDH plates. This evidence supported the XRD results. Among all samples, Ca2Al/SDS/Indigo (Fig. 5d) exhibited the smallest lateral size of plate-like particles resulting in a highest surface area.

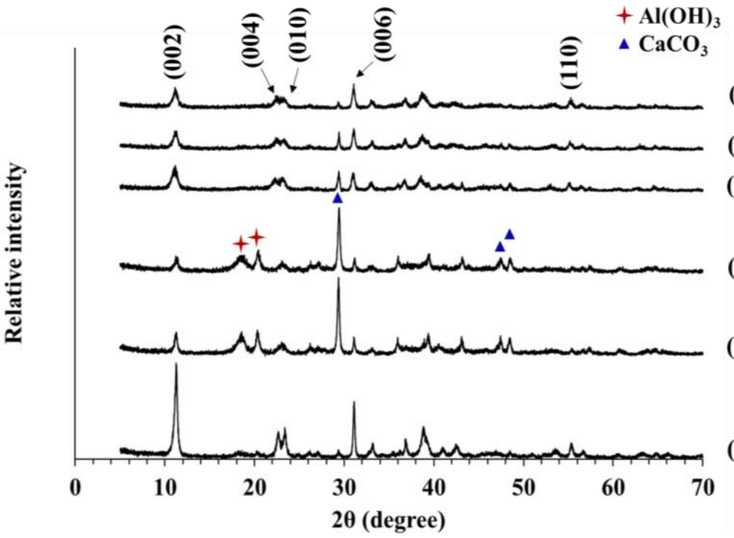

Fig. 3. XRD patterns of (a) Ca2Al/Indigo, (b) Ca3Al/Indigo, (c) Ca4Al/Indigo, (d) Ca2Al/SDS/Indigo, (e) Ca3Al/SDS/Indigo, (f) Ca4Al/SDS/Indigo.

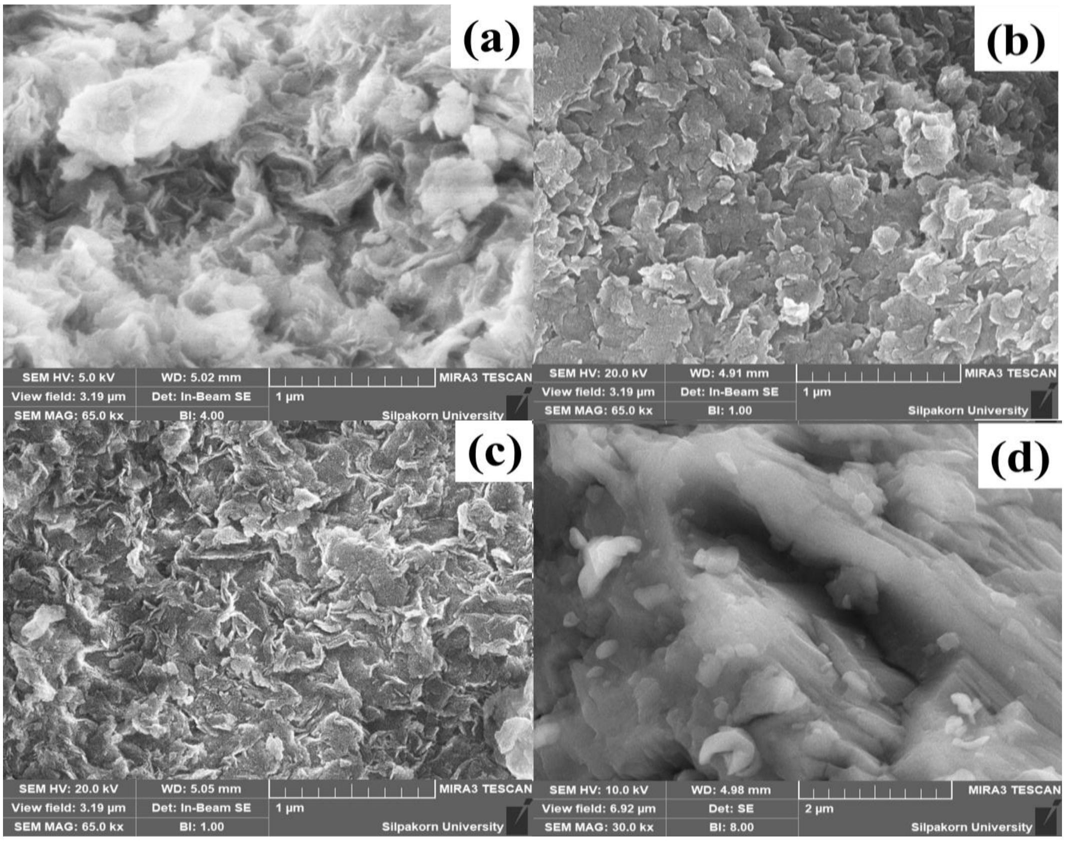

Fig. 4. SEM images of (a) Ca_2Al-LDH, (b) Ca_3Al-LDH, (c) Ca_4Al-LDH and (d) Indigo carmine powder.

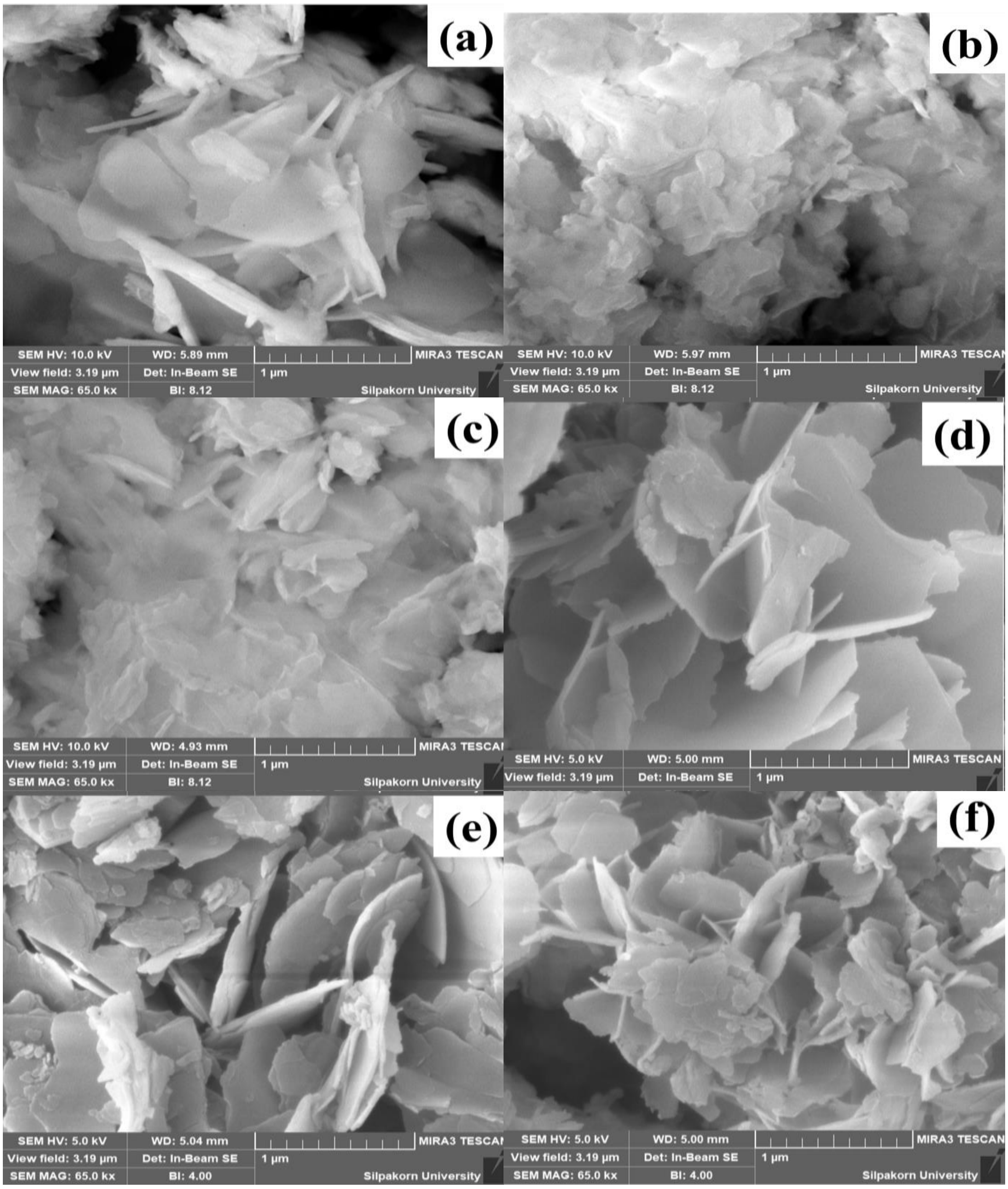

Fig. 5. SEM images of (a) Ca2Al/Indigo, (b) Ca3Al/Indigo, (c) Ca4Al/Indigo, (d) Ca2Al/SDS/Indigo, (e) Ca3Al/SDS/Indigo, (f) Ca4Al/SDS/Indigo.

The FT-IR spectra of the CaAl-LDHs (Fig. 6) showed the O-H stretching of the intercalated water and the surface hydroxyl groups of LDHs at 1639 cm^{-1} and 3449 cm^{-1}. The M-OH stretching of LDHs was found at 495 cm^{-1}. Moreover, the C-O stretchings of intercalated carbonate anions were observed at 1018 cm^{-1} and 1419 cm^{-1}. The FT-IR spectra of the organic modified-LDHs are illustrated in Figure 7. For CaAl/Indigo samples (Fig. 7 (a) – (c)), the characteristic peaks of both CaAl-LDH and indigo carmine dye were clearly observed in their spectra. The additional band at 1613 cm^{-1} was attributed to the C=C stretching of the benzene ring of indigo carmine [20, 21]. For the CaAl/SDS/Indigo materials, the characteristic bands of both were still evident. Furthermore, the addition peaks of SDS were found at 2920 and 2850 cm^{-1} which were assigned to the C – H stretching and those at 1214 and 1063 cm^{-1} were attributed to the S – O stretching. The S – O peaks shifted to a lower wavenumber compared with those of pure SDS. The results suggested that there was interaction between the sulfate groups and the LDH surface [22-24].

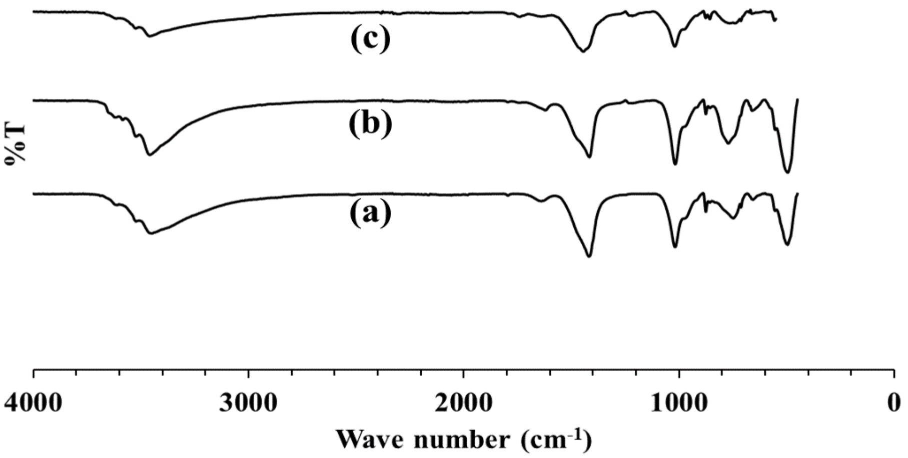

Fig. 6. FT-IR spectra of (a) Ca_2Al-LDH, (b) Ca_3Al-LDH and (c) Ca_4Al-LDH.

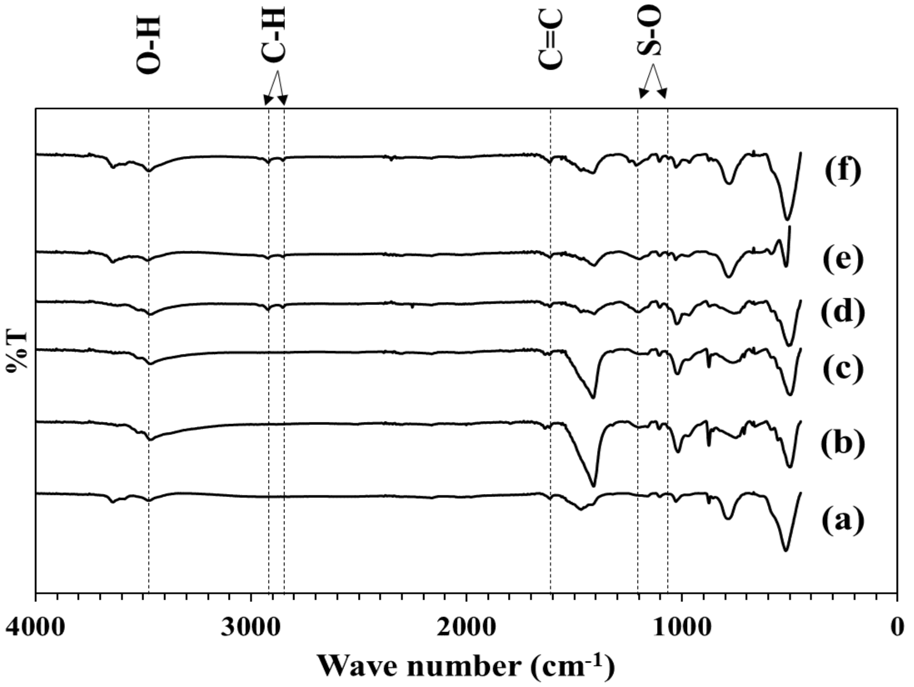

Fig. 7. FT-IR spectra of (a) Ca2Al/Indigo, (b) Ca3Al/Indigo, (c) Ca4Al/Indigo, (d) Ca2Al/SDS/Indigo, (e) Ca3Al/SDS/Indigo, (f) Ca4Al/SDS/Indigo.

4.2. Optical properties

Figure 8 illustrates the absorption spectra of various organic modified CaAl-LDHs with different Ca^{2+}/Al^{3+} ions ratios. The absorption spectrum of pure Indigo carmine (IC) shows broad absorption over the visible range which corresponds to its visual color of dark blue. All the CaAl/Indigo and CaAl/SDS/Indigo samples exhibited the maximum absorption at approximately 610 nm which were attributed to the $n - \pi^*$ transition of the chromophore centers from indigo carmine [25]. The color coordinates of the CaAl/Indigo and CaAl/SDS/Indigo (Table 2) demonstrated that the color of the hybrid pigments was blue. The results revealed that the Ca2Al/SDS/Indigo sample exhibited the most intense blue color due to its microstructure.

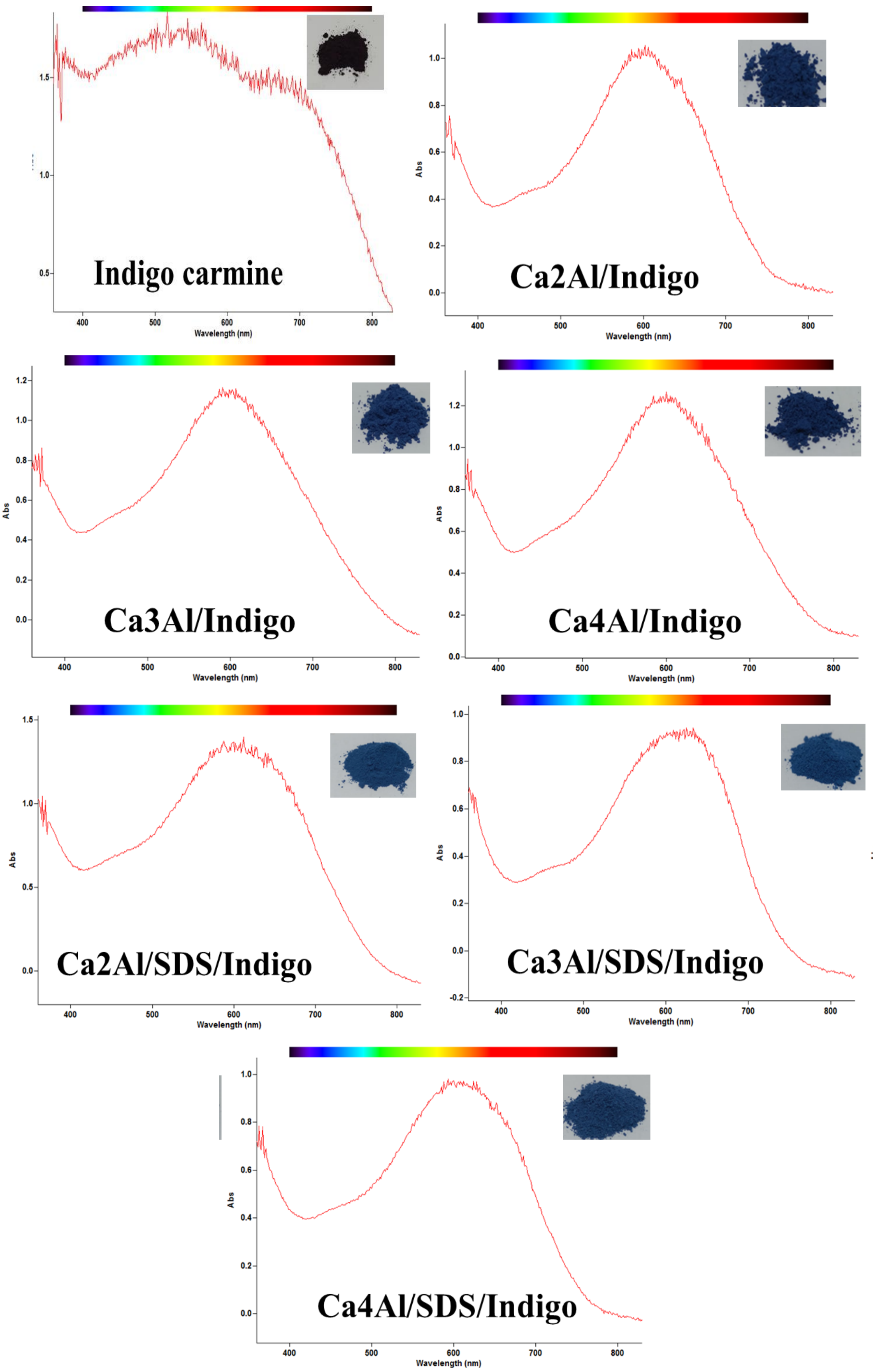

Fig. 8. UV-vis spectra of Indigo carmine and organic modified CaAl-LDHs.

Table 2. The L, a* and b* parameters of CaAl-SDS-LDH/Indigo carmine samples.*

LDH Samples	*L**	*a**	*b**
Ca2Al-LDH	122.28	-0.29	4.57
Ca2Al/Indigo	45.67	-10.95	-36.87
Ca2Al/SDS/Indigo	31.89	-7.84	-33.99
Ca3Al-LDH	123.84	-0.79	4.29
Ca3Al/Indigo	40.22	-7.34	-36.28
Ca3Al/SDS/Indigo	50.06	-14.09	-38.51
Ca4Al-LDH	122.32	-0.64	5.59
Ca4Al/Indigo	36.60	-7.41	-35.53
Ca4Al/SDS/Indigo	46.50	-10.49	-33.31

4.3. Photostability of samples

Powdered samples of the CaAl/Indigo and CaAl/SDS/Indigo were photoaged in a UV photoaging instrument.

Figures 9-10 represent the durability of the above samples against UV irradiation up to 240 h. Accordingly, this study represents high photo-stability. This result suggested that the indigo carmine dye could be protected by the CaAl-LDH sheets from photodegradation. These hybrids CaAl/Indigo and CaAl/SDS/Indigo samples can be considered to be good candidates for colorant hybrid materials.

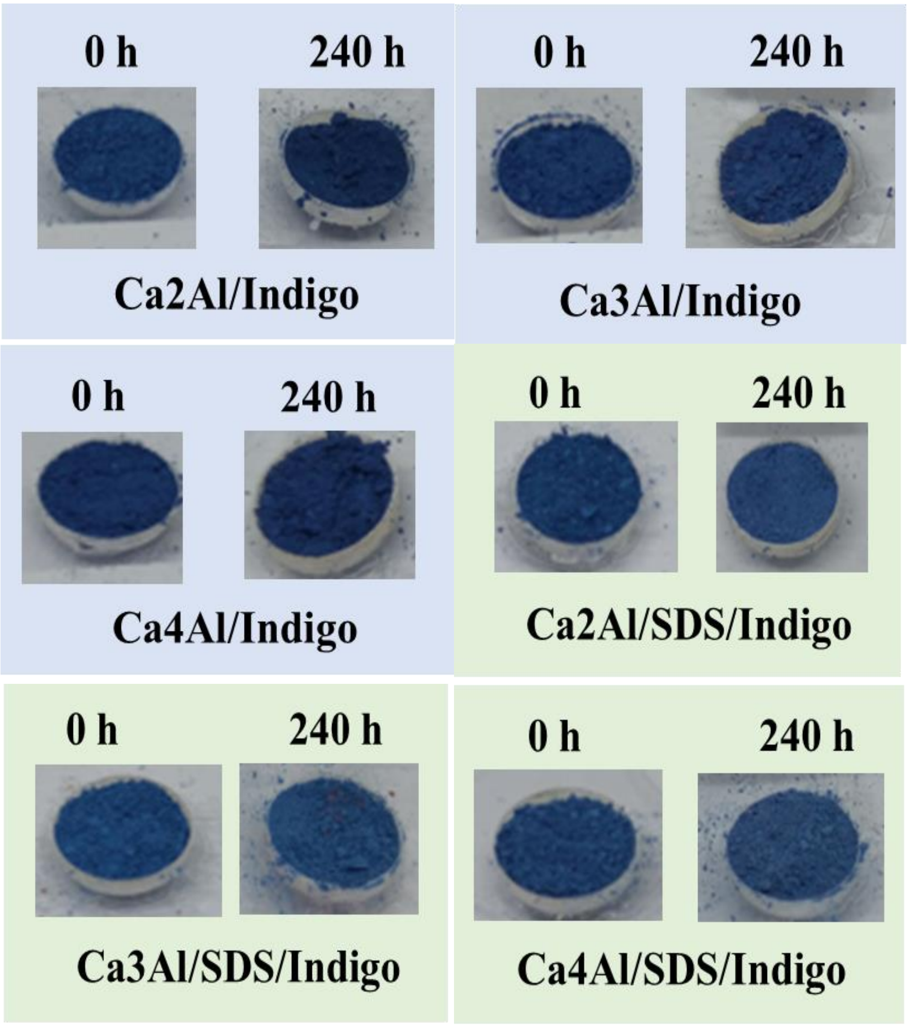

Fig. 9. Photograph of CaAl/Indigo and CaAl/SDS/Indigo under UV irradiation.

The ΔE values of the irradiated CaAl/Indigo and CaAl/SDS/Indigo samples (Fig. 11) were measured up to a total exposure time of 240 h. The ΔE value of the indigo carmine dye changed from 4 to 7 for the CaAl/Indigo and value from 3 to 5 for CaAl/SDS/Indigo samples. The results showed that SDS can reduce the photodegradation of indigo carmine dye by UV radiation.

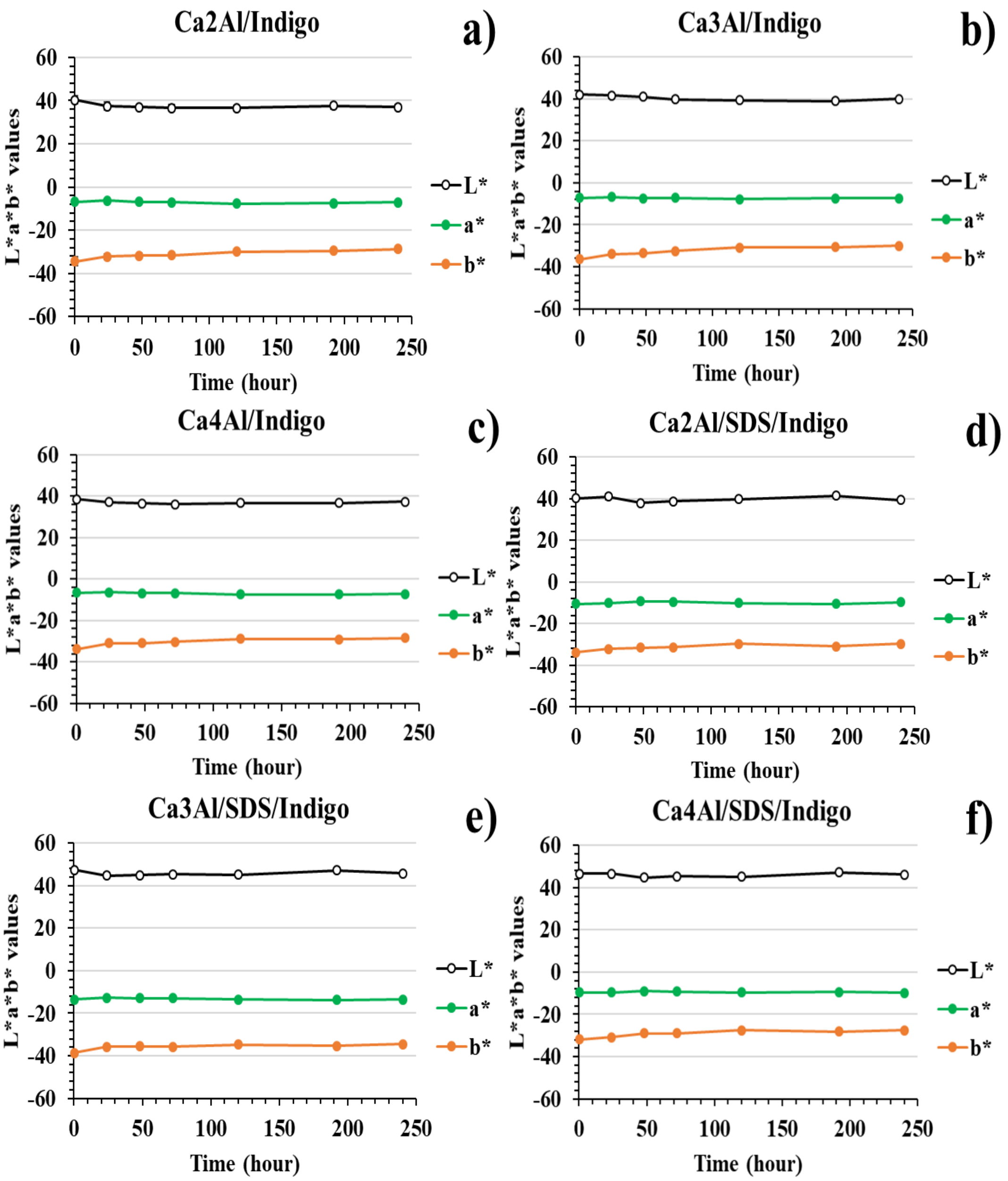

Fig. 10. Stability test of organic modified CaAl-LDHs under UV irradiation.

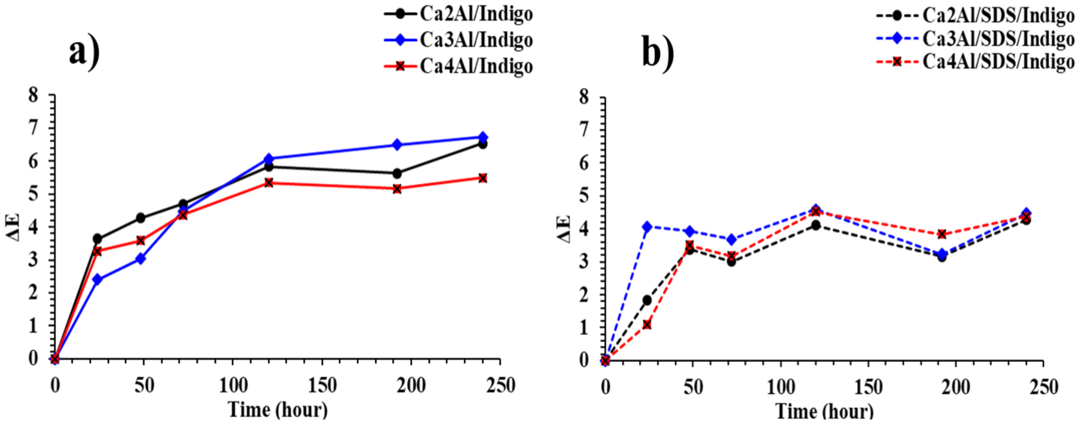

Fig. 11. Color difference (ΔE) values for (a) CaAl/Indigo and (b) CaAl/SDS/Indigo samples as a function of UV aging time.

4.4. Cytotoxicity

The cytotoxicity to GF cells at CaAl-LDH, CaAl/Indigo and CaAl/SDS/Indigo concentrations of 10 - 1000 µg/mL was also examined via the MTT assay. As shown in Figure 12, the cell viabilities of the CaAl-LDH and CaAl/Indigo in the test range were all above 90% at 10-1000 µg/mL while those of the CaAl/SDS/Indigo were 20-60% at 500- 1000 µg/mL, suggesting that these SDS incorporated CaAl-LDHs induced some cytotoxicity. As shown in Figure 9, LDH nanoparticles exhibited no toxicity even at 1000 µg/mL, indicating that LDH is biocompatible to the GF cells.

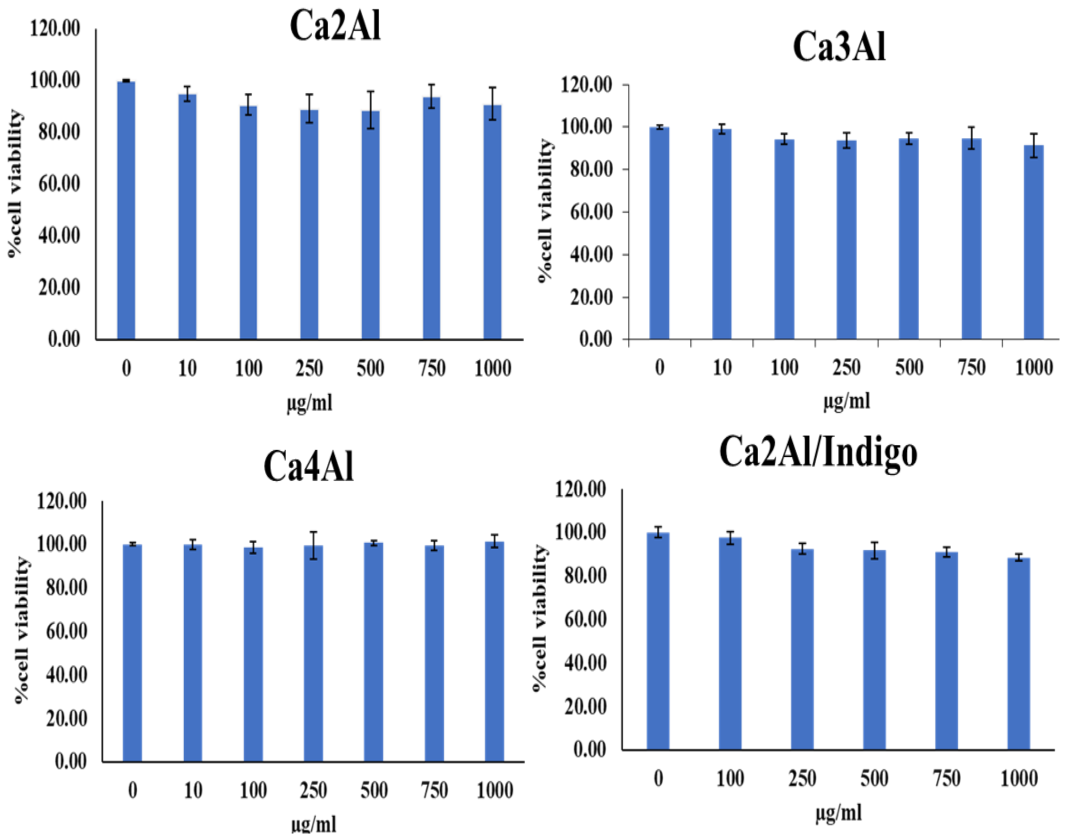

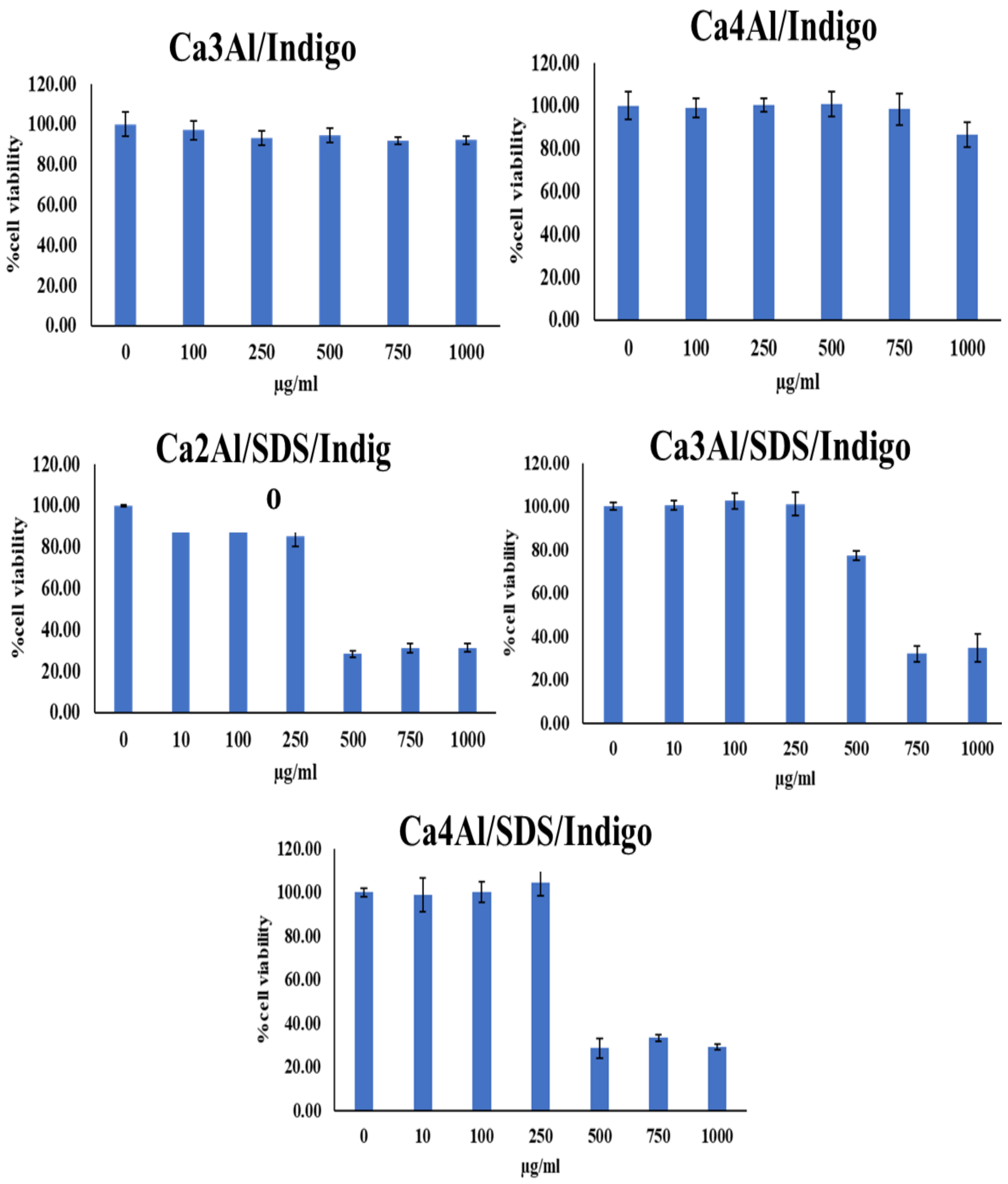

Fig. 12. Cytotoxicity test of (top) CaAl-LDHs, (middle) CaAl/Indigo and (bottom) CaAl/SDS/Indigo samples.

Conclusions

CaAl/Indigo and CaAl/SDS/Indigo composites were successfully prepared by precipitation of CaAl-LDHs in the solution containing indigo carmine dye and sodium dodecyl sulphate. The FE-SEM images revealed that the CaAl/Indigo and CaAl/SDS/Indigo composites had plate-like structure. XRD results showed that CaAl-LDHs were mainly composed of CaAl-hydrotalcites structure. The FT-IR spectra exhibited the characteristic bands of indigo carmine dye and sodium dodecyl sulphate and CaAl-hydrotalcites structure. The absorption spectra of the CaAl/Indigo and CaAl/SDS/Indigo composites exhibited intense blue color. Furthermore, the CaAl/Indigo and CaAl/SDS/Indigo composites exhibited high photo-stability under UV irradiation. The cellular uptake tests showed that most CaAl/Indigo and CaAl/SDS/Indigo composites possessed biocompatibility to the GF cells except the SDS modified CaAl-hydrotalcites structure. In conclusion, these hybrids CaAl/Indigo and CaAl/SDS/Indigo samples can be considered good candidates for colorant hybrid materials.

Acknowledgements

The author would like to thank the Faculty of Science, Silpakorn University, Nakhon Pathom, Thailand for financial support (Grant No. SRIF-PRG-2564-02).

References

[1] A. Marzec, B. Szadkowski, J. Rogowski, W. Maniukiewicz, M. Kozanecki, D. Moszyński, et al., Journal of Industrial and Engineering Chemistry **70**, 427(2019); https://doi.org/10.1016/j.jiec.2018.11.005

[2] B. Szadkowski, A. Marzec, P. Rybiński, W. Maniukiewicz, M. Zaborski, Polymers **11**(1), 43(2019); https://doi.org/10.3390/polym11010043

[3] S. Mandal, D. Tichit, D. A. Lerner, N. Marcotte, Langmuir **25**(18), 10980(2009); https://doi.org/10.1021/la901201s

[4] M. Ogawa, K. Kuroda, Chemical Reviews **95**(2), 399(1995); https://doi.org/10.1021/cr00034a005

[5] S. Yoo, J. S. Hsieh, P. Zou, J. Kokoszka, Bioresource Technology **100**(24), 6416(2009); https://doi.org/10.1016/j.biortech.2009.06.112

[6] H. Hashimoto, J. Kiyohara, A. Isozaki, Y. Arakawa, T. Fujii, J. Takada, et al., ACS Omega **5**(8), 4330(2020); https://doi.org/10.1021/acsomega.9b04297

[7] E. Pérez-Ramírez, E. Lima, A. Guzmán, Dyes and Pigments **120**, 161(2015); https://doi.org/10.1016/j.dyepig.2015.03.040

[8] M. Gupta, N. Pal, A. Tewari, N. Lal, Journal of Electronics and Communication Engineering **15**(5), 7(2020); https://doi.org/10.9790/2834-1505010713

[9] S. M. El-Sawy, N. M. Ahmed, M. A. Abd El-Ghaffar, Egyptian Society of Polymer Science and Technology (Egypt); Academy of Scientific Research and Technology (Egypt); Helwan University (Egypt); National Research Centre (Egypt); Syndicate of Scientific Prokion (Egypt), (2005).

[10] M. Szabados, Z. Kónya, Á. Kukovecz, P. Sipos, I. Pálinkó, Applied Clay Science **174**, 138(2019); https://doi.org/10.1016/j.clay.2019.03.033

[11] B. Wan, Y. Yan, R. Huang, D. B. Abdala, F. Liu, Y. Tang, et al., Sci Total Environ **650**(Pt 2), 1980(2019); https://doi.org/10.1016/j.scitotenv.2018.09.230

[12] J. Wang, T. Zhang, M. Li, Y. Yang, P. Lu, P. Ning, et al., RSC Advances **8**(40), 22694(2018); https://doi.org/10.1039/C8RA03647K

[13] S. S. Shafiei, M. Solati-Hashjin, H. Rahim-Zadeh, A. Samadikuchaksaraei, Advances in Applied Ceramics **112**(1), 59(2013); https://doi.org/10.1179/1743676112Y.0000000045

[14] P. Tang, Y. Feng, D. Li, Dyes and Pigments **90**(3), 253(2011); https://doi.org/10.1016/j.dyepig.2011.01.007

[15] T. H. Kim, J. A. Lee, S. J. Choi, J. M. Oh, International journal of molecular sciences **15**(12), 22563(2014); https://doi.org/10.3390/ijms151222563

[16] C. A. Lapp, G. S. Schuster, Journal of Biomedical Materials Research **60**(1), 30(2002); https://doi.org/10.1002/jbm.10057

[17] P. Zhang, M. Xiang, P. Li, S. Ouyang, T. He, Q. Deng, Environmental Science and Pollution Research **26**, (2019); https://doi.org/10.1007/s11356-019-05295-8

[18] A. A. A. Ahmed, Z. A. Talib, M. Z. Hussein, Journal of Nanomaterials **2013**, 639354(2013); https://doi.org/10.1155/2013/639354

[19] C. X. Jia, S. P. Li, H. Zhong, Journal of Dispersion Science and Technology **32**(4), 604(2011). https://doi.org/10.1080/01932691003757405

[20] S. Ben Younes, C. Dallali, A. Ellafi, L. Bouslama, A. Feriani, S. Sayadi, Catalysis Letters **151**(5), 1248(2021).

[21] E. Ortiz, V. Gómez-Chávez, C. M. Cortés-Romero, H. Solís, R. Ruiz-Ramos, S. Loera-Serna, Journal of Environmental Protection **7**, 1693(2016); https://doi.org/10.4236/jep.2016.712137
[22] W. G. Dai, L. C. Dong, International Journal of Pharmaceutics **336**(1), 58(2007); https://doi.org/10.1016/j.ijpharm.2006.11.035
[23] A. Elsayed, M. Al-Remawi, N. Qinna, A. Farouk, K. A. Al-Sou'od, A. A. Badwan, AAPS PharmSciTech **12**(3), 958(2011); https://doi.org/10.1208/s12249-011-9647-5
[24] E. M. van der Merwe, C. L. Mathebula, L. C. Prinsloo, Powder Technology **266**, 70(2014); https://doi.org/10.1016/j.powtec.2014.06.008
[25] N. Hareesha, J. G. Manjunatha, B. M. Amrutha, P. A. Pushpanjali, M. M. Charithra, N. Prinith Subbaiah, Journal of Electronic Materials **50**(3), 1230(2021); https://doi.org/10.1007/s11664-020-08616-7